図表３　地方公共団体等における有害大気汚染物質モニタリングの対象物質

・揮発性有機化合物：ベンゼン，トリクロロエチレン，テトラクロロエチレン，ジクロロメタン，アクリロニトリル，塩化ビニルモノマー，クロロホルム，1,2-ジクロロエタン，1,3-ブタジエン，酸化エチレン
・アルデヒド類：アセトアルデヒド，ホルムアルデヒド
・多環芳香族炭化水素：ベンゾ[a]ピレン
・金属類：水銀及びその化合物，ニッケル化合物，ヒ素及びその化合物，ベリリウム及びその化合物，マンガン及びその化合物，クロム及びその化合物

3. 環境モニタリング事業からわかること

わが国の環境管理は，公害を克服するという歴史的経緯もあり環境基準の達成を一つの目標として進められている。従って，わが国は世界的に見て環境モニタリングに熱心である。そのような背景の下，19種類の有害化学物質（図表３）の環境モニタリングが，1997年度より大気汚染防止法に基づいて地方公共団体により行われている。

その結果は興味深いものである。ベンゼンの大気環境基準値はその発癌リスクに基づいて3$\mu g/m^3$と定められている。一般環境中では環境基準値はほぼ達成されているが，道路沿道では達成されていない地点が多いことがわかる（図表４Ａ）。勿論，環境基準値はこの濃度のベンゼンを一生にわたって吸い続けたとき，10万人に１人が癌を発症すると予測される値に近いものであり，環境基準を若干超えたとしても，にわかに重大な健康影響が発生するものではない。しかしながら，より重点的な対策が必要であることはいうまでもない。

強い変異原性が知られ，動物実験で発癌性が確認されているベンゾ[a]ピレン（図表６）はしばしば大気中に検出される化学物質である。環境基準値は定められていないが，発生源周辺や道路沿道では特異的に濃度が高い観測点が知られる（図表４Ｂ）。大気中に存在する化学物質の変異原性を考えたとき，留意すべき知見である。

4. バイオモニタリングの意義

上記のように環境中には数多くの種類の化学物質が存在する。そのリスク評価は大きな課題であり，社会的意義は大きい。化学物質のリスクは

[リスク]＝[化学物質の有害性]×[曝露量]

として，しばしば概念的に定式化される。[化学物質の有害性]は化学物質固有の値であり，[曝露量]は地域固有の値である。このことは一般論としては正しい。一方，現実の環境を考えたとき，環境中にはおそらく100種類以上の化学物質が存在するため，そのリスクは各々の化学物質のリスクの総和として

$$[\text{リスク}]=[\text{化学物質の有害性}]_1\times[\text{曝露量}]_1+[\text{化学物質の有害性}]_2\times[\text{曝露量}]_2+\cdots+[\text{化学物質の有害性}]_n\times[\text{曝露量}]_n$$

$n>100$

のように表現されることが期待されるが，そう簡単なものではない。よく考えてみると，地域ごとにまったく同じ化学物質が存在することはありえず，また，すべての化学物質の有害性が明らかにされているわけではない。従って，化学物質の有害性を同定し，その曝露量を推定

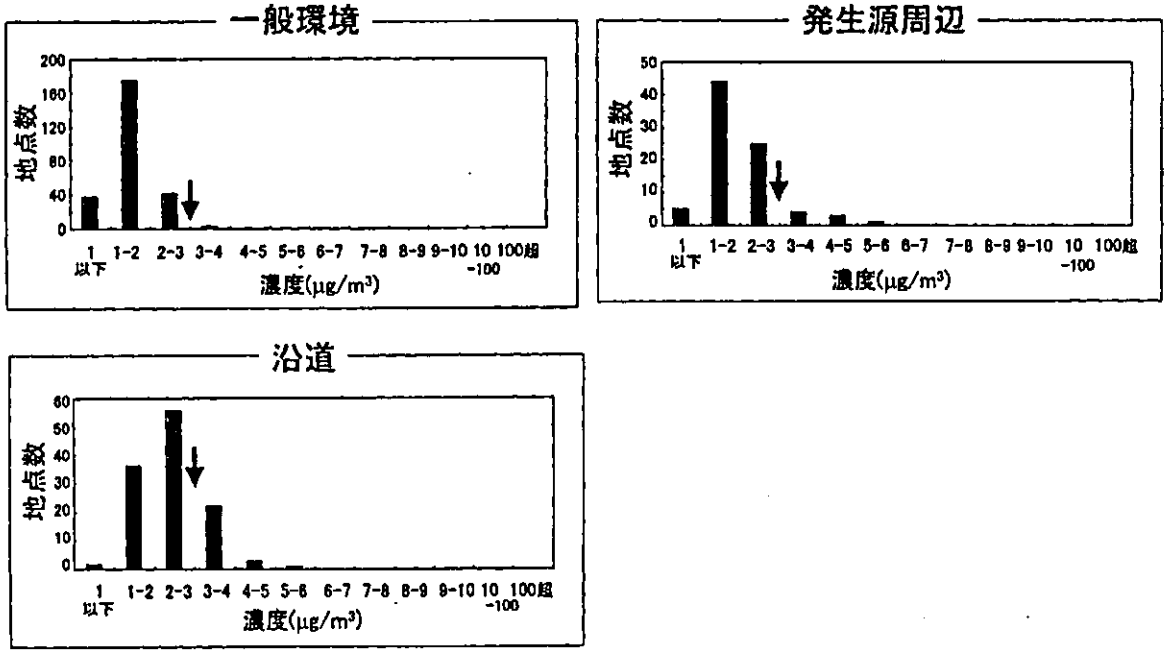

図表４Ａ　有害大気汚染物質モニタリング－ベンゼンの一般大気中濃度（2003年度）（環境省ホームページより引用）

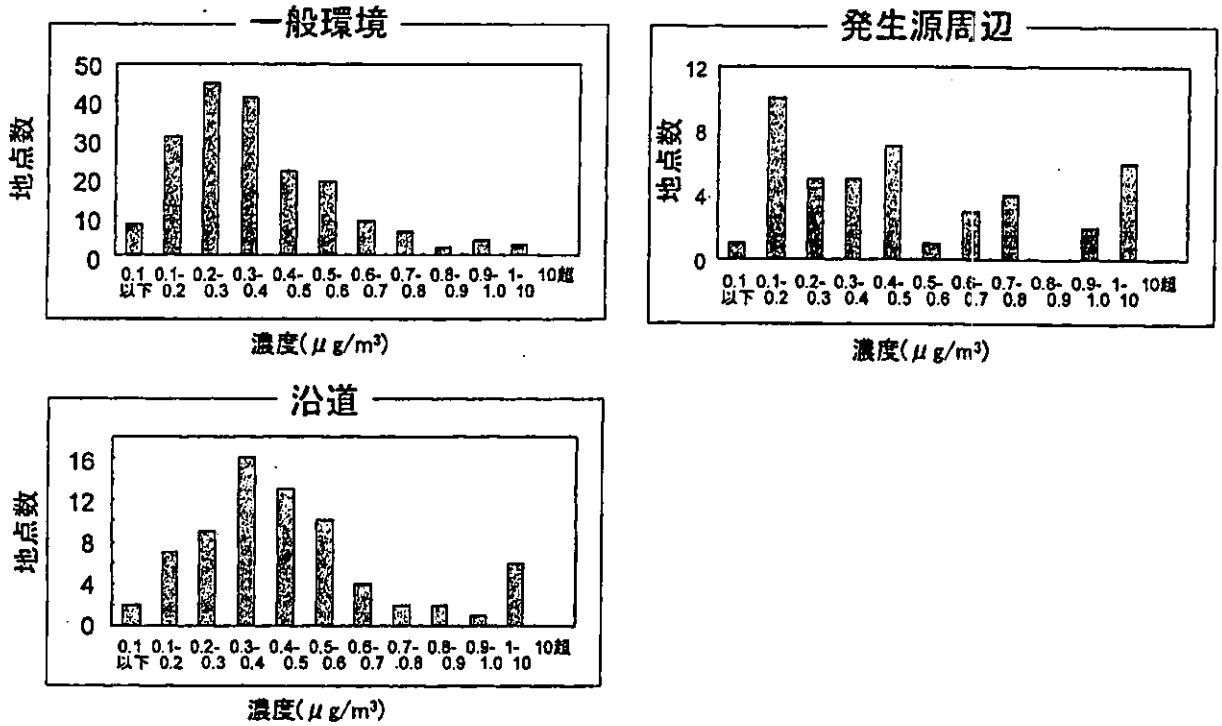

図表4B　有害大気汚染物質モニタリング－ベンゾ[a]ピレンの一般大気中濃度(2001年度)(環境省ホームページより引用)

するアプローチのみでは，環境からの化学物質曝露によるリスクの評価が十分可能になるとはいえない。

現在行われている化学物質の排出量把握や個々の化学物質の機器分析によるモニタリングを補完する手法の一つとして，バイオアッセイによる環境モニタリングが考えられる。環境から生体に与えられるインパクトの総体をバイオアッセイにより定量化することで，化学物質の複合曝露のリスクを評価しようとするアプローチである。最も洗練されているバイオアッセイ手法は，化学物質が遺伝子に突然変異を引き起こす性質(変異原性)をサルモネラなどの細菌を用いて検出・定量する方法であり，この方法は開発者の名前をとってエームス法と呼ばれている。

5. 細菌による変異原性モニタリングから判ったこと

変異原性を示す化学物質は変異原物質と総称され，その多くは発癌性を示す。人の健康の観点からは，環境中に存在する化学物質がどの程度の変異原性を示すかをバイオアッセイによりモニタリングし，明らかにしておく必要がある。実際，わが国の大気や水環境からは，ディーゼル機関の排気を主な排出源とするベンゾ[a]ピレンやニトロピレン類(図表5)などの変異原物質が検出されている。そこで河川水や大気粉塵あるいは土壌を採取し，そこに含まれる化学物質の変異原性がエームス法を用いて定量されてきた。例えば，大気中の浮遊粒子状物

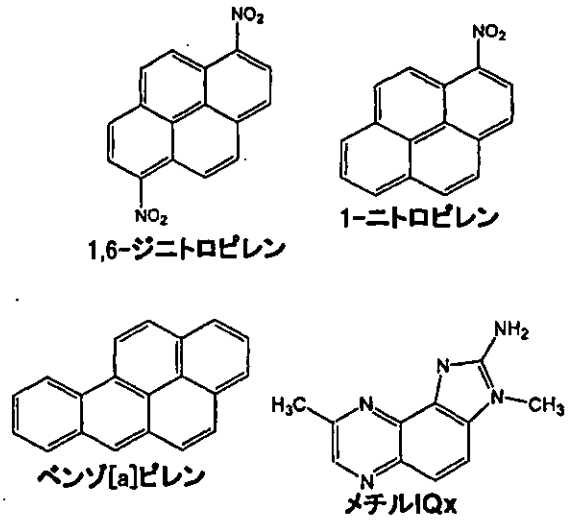

図表5

質が示す変異原性の粒子径分布が，東京都内をフィールドとして調べられている。粒子径1ミクロン以下の分画に高い変異原性が認められることに興味が持たれる(図表6)。

環境省の事業としてもエームス法を活用した環境中の変異原物質の調査が，全国で行われている。その結果，新規の変異原物質が見出された事例も知られている。例えば，京都・桂川水系の河川水から高い変異原性を持つ化学物質が検出され，それがPBTAと呼ばれる一連の

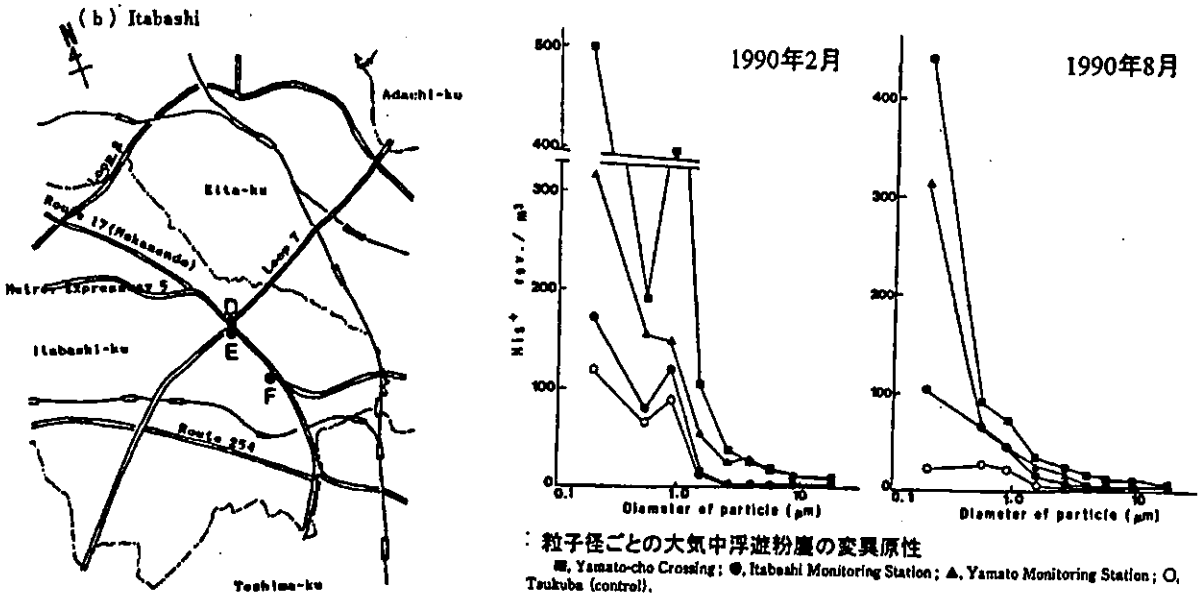

：粒子径ごとの大気中浮遊粉塵の変異原性

■, Yamato-cho Crossing; ●, Itabashi Monitoring Station; ▲, Yamato Monitoring Station; ○, Tsukuba (control).

図表6　大気中浮遊粒子状物質中の変異原物質(松本，安藤，田村　衛生化学39，139(1993)より引用)

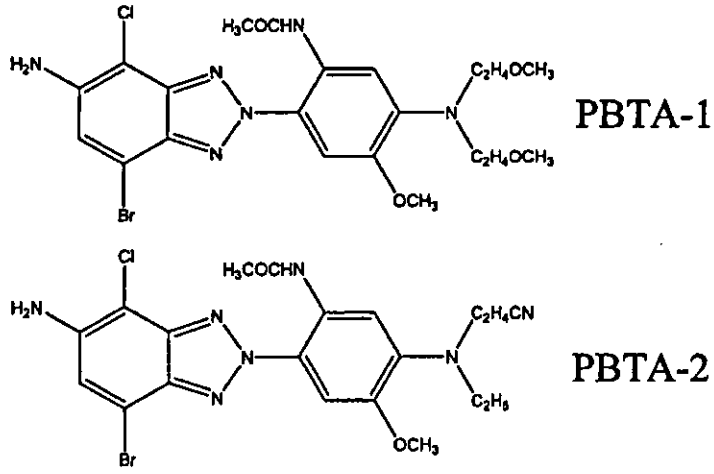

図表7

化合物(図表7)であると同定された。これらの化合物はアゾ色素の変化体であることが明らかとなったが，その後，他の河川でも同様の変異原物質の検出が報告されている。また，土壌中からは，ニトロピレン類ばかりでなく，高い変異原性をもつ様々のニトロ化された多環芳香族炭化水素が検出されている。その排出源は明らかにされていない。

6. 動物個体を用いた変異原物質の検出

環境中には高い変異原性を持つ化学物質が存在することが，エームス法を用いて明らかにされてきた。しかし，変異原物質の健康影響を考えたとき，私たちが本当に知りたいことは，高い変異原性をもつ化学物質が環境から人に取り込まれたとき，どの程度の頻度で遺伝子上に突然変異が発生するか，さらに癌が発生するかを明らかにすることである。しかし，エームス法はあくまで細菌中で発生する突然変異を検出する方法である。環境中に存在する化学物質が体内で示す突然変異を検出するには，細菌でなく実験動物を用いる必要がある。

遺伝情報は遺伝子の本体であるDNA上で，アデニン(A)，チミン(T)，グアニン(G)，シトシン(C)という4種類の塩基と呼ばれる分子の配列でコード(記録)されているが，突然変異とはDNA上の塩基分子の配列が変化してしまうことである。変異原物質は塩基分子に結合して，塩基分子の配列を変換する性質を持っている。例えば，ベンゾ[a]ピレンはGをTに変換する突然変異をよく引き起こす。サルモネラを変異原物質で処理すると様々の突然変異が引き起こされる。エームス法の場合，突然変異の結果引き起こされるサルモネラの性質の変化を利用して突然変異の発生頻度を調べるが，最も多用されるのが，ヒスチジンというアミノ酸の一種がないと増

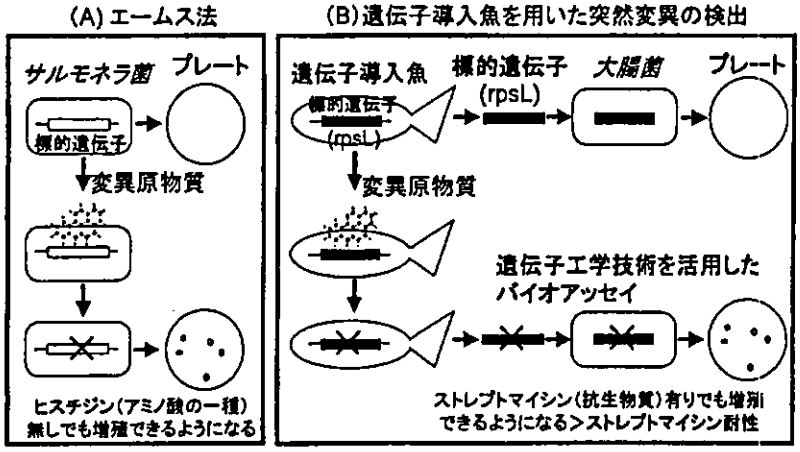

図表8　エームス法(A)と遺伝子導入ゼブラフィッシュを用いた変異原物質検出法の比較(青木，天沼　用水と排水46(12)，3(2004)より引用)

殖できないサルモネラが，ヒスチジンがなくても増殖できるようになるというサルモネラの性質の変化である。実際には，化学物質でサルモネラを処理した後，ヒスチジンを含まない寒天培地上で増殖できるサルモネラが発生する頻度を調べ，化学物質の変異原性の強さを評価する(図表8 A)。

その一方，動物体内で発生する突然変異を定量的に検出することは長年困難であった。しかし，遺伝子工学技術の進歩に伴い，化学物質の変異原性を検出するための標的遺伝子を遺伝子導入した動物が作成できるようになり，これが可能となった。変異原性検出用に開発された遺伝子導入動物(ゼブラフィッシュやラット・マウス)に化学物質を曝露し，化学物質が動物体内で示す変異原性を検出する手法の研究が精力的に進められている。

7. 変異原物質検出用遺伝子導入ゼブラフィッシュの開発

私たちの研究室では，水環境中に存在する化学物質の変異原性を検出するための遺伝子導入ゼブラフィッシュ(体長2～3cmの淡水性熱帯魚，図表9)を世界に先駆けて開発している。私たちの遺伝子導入ゼブラフィッシュのDNAには，突然変異を検出する標的遺伝子として大腸菌のストレプトマイシン(抗生物質)感受性決定遺伝子 *rpsL* のDNAが導入されている。この遺伝子導入魚を変異原物質で処理すると，変異原物質が魚の体内で *rpsL* 遺伝子DNAに結合して突然変異が発生する。*rpsL* 遺伝子DNAが魚の体内に存在したままでは突然変異を検出できないので，*rpsL* 遺伝子DNAを大腸菌に遺伝子導入するが，*rpsL* 遺伝子は元々大腸菌の遺伝子なので，大腸菌の性質を変えることができる。突然変異がない無傷の *rpsL* 遺伝子DNAが導入された大腸菌はストレプトマイシンに感受性になるのに対して，突然変異が発生した *rpsL* 遺伝子DNAが導入された大腸菌

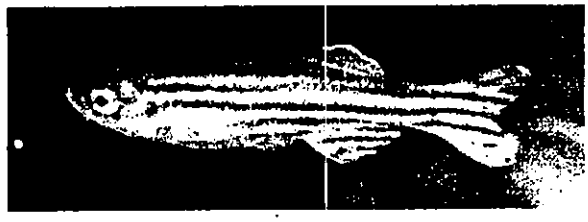

図表9　ゼブラフィッシュ

はストレプトマイシンに耐性となり，ストレプトマイシンを含む寒天培地上でも増殖できる。このストレプトマイシン耐性大腸菌の発生頻度から，魚体内での突然変異発生頻度を知ることができる。

現在この遺伝子導入ゼブラフィッシュの胚や成魚を用いて，変異原物質が体内で引き起こす突然変異が検出できることの検証実験をすすめている。例えば，アルキル化剤であり強い変異原物質である *N*-メチル-*N'*-ニトロ-*N*-ニトロソグアニジン(MNNG)の変異原性が，遺伝子導入ゼブラフィッシュの胚をこの化合物で処理することにより検出可能である(図表10)。また，MNNGで成魚を処理すると，エラや膵・肝臓(ゼブラフィッシュでは膵臓と肝臓は同じ臓器になっている)で突然変異が発生していた。また，遺伝子導入ゼブラフィッシュ胚を用いてベンゾ[a]ピレンや肉の焼け焦げに含まれるヘテロサイクリックアミンであるMeIQx(図表5)による突然変異が検出できた。

8. 大気中の変異原物質が肺で示す変異原性

大気中に多くの化学物質が排出されている現状を考えると，大気中の化学物質が発揮する変異原性の評価は重要である。大気汚染の影響が最も強く現れる器官は呼吸器，特に肺である。私たちの研究室では変異原物質検出用マウスを用いて大気汚染物質が肺で示す変異原性の評価を進めている。私たちは *gpt* デルタマウスという国立医薬品食品衛生研究所の能美健彦博士により開発された

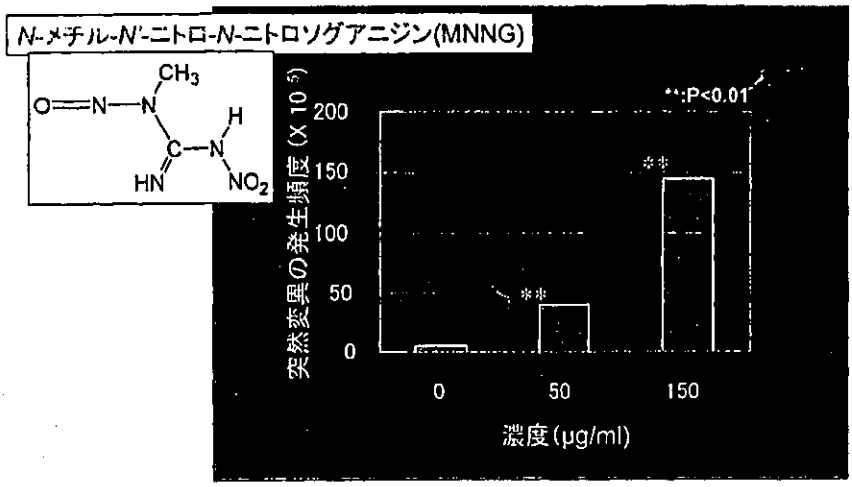

図表10　遺伝子導入ゼブラフィッシュ胚を用いたN-メチル-N'-ニトロ-N-ニトロソグアニジン(MNNG)による突然変異の検出(青木，天沼　用水と排水46(12)，3(2004)より引用)

マウスを用いている。このマウスを用いることにより，遺伝子導入ゼブラフィッシュとほぼ同様の原理で，動物体内に発生した突然変異を検出することができる。

前述のように，ベンゾ[a]ピレンは大気中にしばしば検出される変異原物質である。このベンゾ[a]ピレンを気管から *gpt* デルタマウスの肺中に投与すると，投与量に依存して直線的に突然変異の発生頻度の増加が認められた。また，国立環境研究所に設置されているディーゼル排気曝露装置内で *gpt* デルタマウスを長期間飼育すると，曝露期間に依存して肺中の突然変異発生頻度が増加した。変異原物質検出用遺伝子導入マウスも環境中に存在する化学物質の変異原性を評価するために利用可能であることが明らかになった。

9. これからの研究

環境中に存在するような低い濃度レベルの化学物質が示す変異原性は，遺伝子導入ゼブラフィッシュやマウスへ長期間の曝露を実施することにより検出可能と考えている。最終的には実際の河川水や大気を曝露して，環境中の化学物質が示す変異原性を検出できるよう技術的問題を解決しようと考えている。

変異原物質の多くが発癌性を持つことはよく知られている。しかし，化学物質の変異原性の強さと発癌性の強さの関係は定量的に明らかになっているわけではない。化学物質の曝露と影響(この場合は発癌)の関係を定量的に把握できるようになって，リスク評価はその威力を発揮する。そのような中，突然変異の発生頻度と癌の発生率の関係を定量的に評価する数理モデルの研究・開発が大きく進んでいる。化学物質が動物体内で示す変異原性の強さから，癌の発生確率を予測できるようになるのも，そう遠い将来のことではないと信じている。環境中に存在する化学物質が総体として示す変異原性を検出するため，本稿で紹介した遺伝子導入動物は優れたツールである。これらの動物を用いたバイオアッセイが環境モニタリングに新しい局面を開くものとして期待している。

(日環協環境セミナー全国大会　特別講演)

J Neurophysiol 92: 2413–2427, 2004.
First published May 19, 2004; 10.1152/jn.00236.2004.

Topographic Representation of Odorant Molecular Features in the Rat Olfactory Bulb

Yuji K. Takahashi,[1] Masahide Kurosaki,[2] Shuichi Hirono,[2] and Kensaku Mori[1]
[1]*Department of Physiology, Graduate School of Medicine, University of Tokyo, Tokyo 113-0033;* [2]*School of Pharmaceutical Sciences, Kitasato University, Tokyo 108-8641, Japan*

Submitted 9 March 2004; accepted in final form 11 May 2004

Takahashi, Yuji K., Masahide Kurosaki, Shuichi Hirono, and Kensaku Mori. Topographic representation of odorant molecular features in the rat olfactory bulb. *J Neurophysiol* 92: 2413–2427, 2004. First published May 19, 2004; 10.1152/jn.00236.2004. Individual glomeruli in the mammalian olfactory bulb (OB) most probably represent a single odorant receptor (OR). The assembly of glomeruli thus forms the maps of ORs. How is the approximately 1,000 ORs represented spatially in the glomerular map? Using the method of optical imaging of intrinsic signals and systematic panels of stimulus odorants, we recorded odorant-induced glomerular activity from the dorsal and dorsolateral areas of the rat OB, and examined the molecular receptive range (MRR) of individual glomeruli. We then deduced the characteristic molecular features that were shared by odorants effective in activating individual glomeruli. Analysis of the spatial representation of the MRR showed that glomeruli with similar MRRs gathered in close proximity and formed molecular feature clusters and subclusters. Although the shape of the clusters varied among different OBs, the clusters were arranged at stereotypical positions in relation to the zonal organization of the OB. Examination of the spatial representation of the characteristic molecular features of odorants using structurally semirigid aromatic compounds suggest a systematic and gradual change in the characteristic molecular features according to the position of subclusters in the map. The topographic map of the characteristic molecular features may reflect a systematic spatial representation of the ORs and may participate in the neural bases for the odorant structure–odor quality relationship.

INTRODUCTION

Mammalian olfactory bulb (OB) has a cortical structure and contains a few thousand glomerular modules (Mori et al. 1999; Shepherd and Greer 1998). Individual glomeruli most probably represent a single odorant receptor (OR; Mombaerts et al. 1996; Ressler et al. 1994; Vassar et al. 1994). Thus the glomerular sheet of the mouse OB forms the maps of approximately 1,000 ORs. How are the numerous ORs represented spatially in the glomerular maps?

Spatial arrangement of OR-representing glomeruli is a crucial determinant for the map of odorant-evoked activity in the OB (Johnson et al. 1998; Leon and Johnson 2003; Meister and Bonhoeffer 2001; Rubin and Katz 1999; Uchida et al. 2000; Xu et al. 2003). The spatial pattern of the odorant-evoked glomerular activity in the mammalian OB has been analyzed with several different methods including 2-deoxyglucose uptake (Coopersmith et al. 1986; Johnson et al. 1998; Royet et al. 1987; Stewart et al. 1979), optical imaging of intrinsic signals (Meister and Bonhoeffer 2001; Rubin and Katz 1999; Uchida et al. 2000), Ca^{2+} imaging (Fried et al. 2002; Wachowiak and Cohen 2001), voltage-sensitive dye imaging (Spors and Grinvald 2002), and functional magnetic resonance imaging (fMRI; Xu et al. 2003; Yang et al. 1998).

These studies began to reveal the basic plan for the spatial organization of the OR maps. For example, glomeruli responsive to structurally similar odorants are clustered in specific regions of the OB (Imamura et al. 1992; Inaki et al. 2002; Leon and Johnson 2003; Meister and Bonhoeffer 2001; Uchida et al. 2000). However, it is not well understood how the represented ORs are spatially arranged in the glomerular maps of the OB.

To further analyze the spatial organization of the glomerular OR maps, we used the method of optical imaging of intrinsic signals that allowed us to measure the response to many (~70) different odorants in a single rat OB and thus to examine the range of odorants that activated individual glomeruli. For the initial mapping study, we used a large panel of odorants (72 different odorants) with a systematic variation of their molecular structure. By comparing the molecular structure of odorants that were effective in activating individual glomeruli, we deduced the characteristic molecular features that the effective odorants shared. We then mapped the characteristic molecular features on the glomerular sheet of the OB.

Because aromatic compounds such as phenols have semirigid molecular conformations, they are more suitable for the estimation of the characteristic molecular features than the open-chain aliphatic compounds, which can have various flexible conformations. In the latter part, we thus focused on the glomeruli in the cluster responsive to phenols and neighboring subclusters, and estimated the spatial representation of the characteristic molecular features. The results suggest the presence of a systematic topographical map of the characteristic molecular features in the dorsal zone of the OB.

METHODS

Animal preparation

Seventeen male Sprague–Dawley rats (200–300 g) were anesthetized with medetomidine [0.5 mg/kg, intraperitoneally (ip)], ketamine (67.5 mg/kg, ip), and pentothal sodium (25 mg/kg, ip). In addition, lactated Ringer solution (0.3 ml/h), containing glucose (25 mg/h), dexamethason (0.02 mg/h), and riboflavine phosphate (0.05 mg/h), was intravenously injected through the tail vein. Rats were mounted in a handmade stereotaxic apparatus that enables us to fix the animal's

Address for reprint requests and other correspondence: K. Mori, Department of Physiology, Graduate School of Medicine, University of Tokyo, 7-3-1 Hongo, Bunkyo-ku, Tokyo 113-0033, Japan (E-mail: moriken@m.u-tokyo.ac.jp).

The costs of publication of this article were defrayed in part by the payment of page charges. The article must therefore be hereby marked "*advertisement*" in accordance with 18 U.S.C. Section 1734 solely to indicate this fact.

odorants and the limited time for the successful recording of glomerular responses (typically 6–8 h), we did not examine the effects of odorant concentration in the present experiments.

Estimation of the characteristic molecular features

In the third series of the experiments, we used for stimulus odorants a panel of aromatic compounds (having a benzene ring), including phenol and its derivatives (Fig. 5). Using Chem3D Ultra (version 7.0, CambridgeSoft, Cambridge, MA), we obtained the 3D structures of the aromatic compounds that were effective in activating individual glomeruli. We then estimated the characteristic molecular features of odorants by superimposing the 3D structures of the effective odorants. Because these compounds have semirigid structures, the most stable conformations were used for the molecular superposition. The superposition of the 3D structure of the compounds was performed by

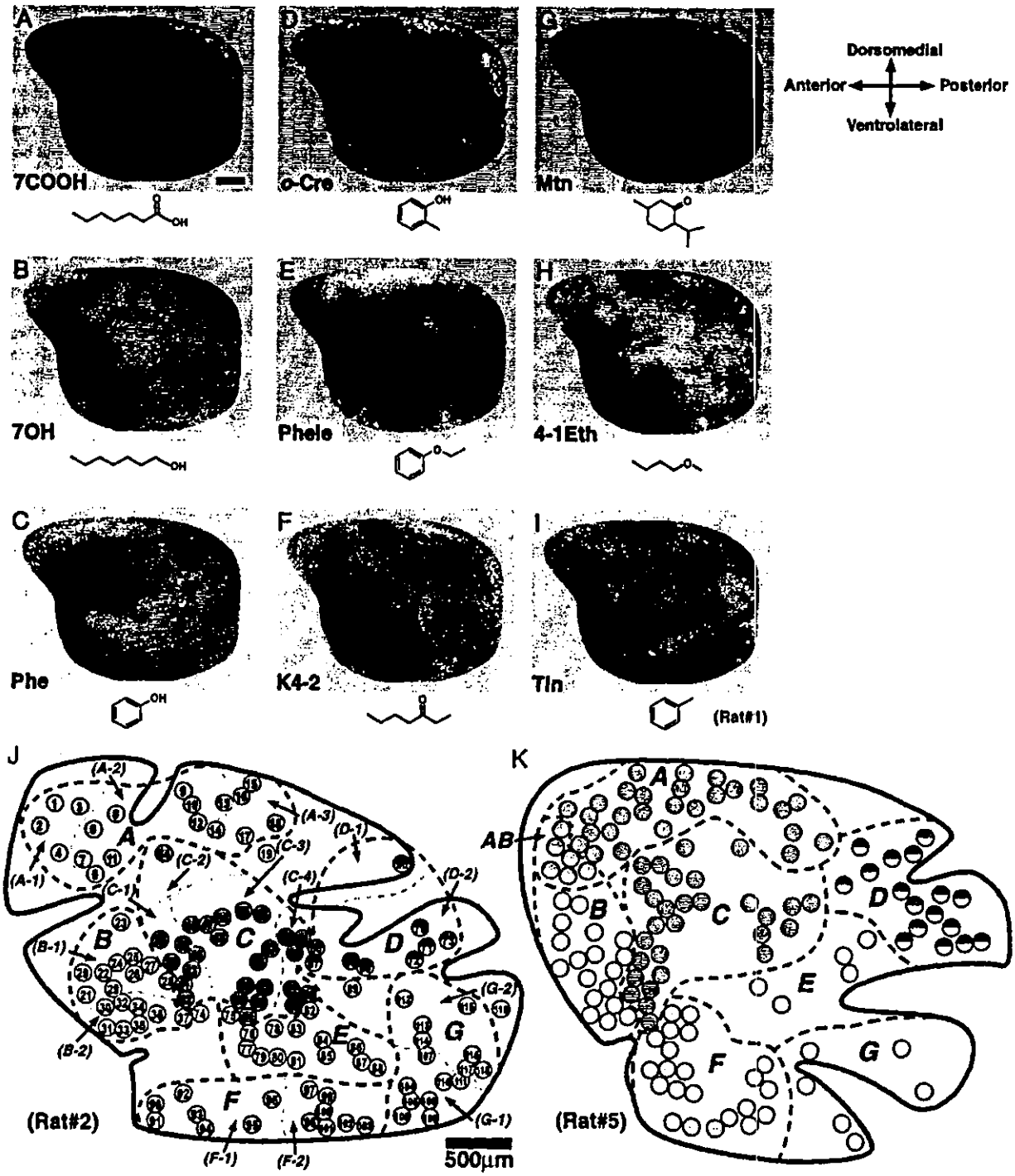

least-square fitting (SYBYL version 6.9 software, Tripos, St. Louis, MO). Because of the flat-sheet structure of the benzene ring, the superimposed 3D structures were represented in 2-dimensional (2D) models (see Fig. 6).

RESULTS

To deduce the characteristic molecular features that are shared by odorants effective in activating individual glomeruli, it is necessary to determine the molecular receptive range (MRR; Mori and Yoshihara 1995) of individual glomeruli. Using a CCD camera that was positioned to image a wide area covering the dorsal and dorsolateral parts of the OB, we recorded glomerular responses to a large and systematic panel of odorants and determined the MRR of individual glomeruli. Figure 1 shows the panel of 72 odorants that were used in the first series of optical imaging experiments (5 rats). The panel consists of 12 structural classes of odorants: 6 aliphatic acids (shown red), 4 aldehydes (pink), 9 aliphatic alcohols (6 primary alcohols and 3 secondary alcohols, yellow), 3 cyclic alcohols (light brown), 7 phenols (green), 5 phenyl ethers (yellow green), 2 diketones (dark brown), 15 aliphatic ketones (blue), 3 aliphatic–aromatic ketones (dark blue), 10 cyclic ketones (pale blue), 3 ethers (purple), and 5 hydrocarbons (gray).

Figure 2, *A–I* show examples of optical images of intrinsic signals that were induced by the stimulation of olfactory epithelium with heptanoic acid (*A*, 7COOH), heptanol (*B*, 7OH), phenol (*C*, Phe), *o*-cresol (*D*, *o*-Cre), phenetole (*E*, Phele), butyl ethyl ketone (*F*, K4-2), menthone (*G*, Mtn), butyl methyl ether (*H*, 4-1Eth), and toluene (*I*, Tln). They were recorded from the OB of the same rat (Rat#1). Odorant-induced intrinsic signals consisted of either isolated spots or larger areas with relatively diffuse darkening. Within the large area, multiple peaks of darkening signal were usually observed. In the present study, we assumed that each isolated spot or each isolated peak in the larger area corresponded to the activity of a single glomerulus (Belluscio and Katz 2001). These records exemplify that each odorant activated a specific combination of glomeruli that were typically clustered in particular regions of the OB. Figure 2, *C* and *D* exemplify that structurally similar odorants activated a largely overlapping but slightly different combination of glomeruli. Figure 2*J* shows the position of 119 glomeruli (numbered from 1 to 119) that responded to at least one of the 72 odorants in the OB of another rat (Rat#2).

Clusters and subclusters of glomeruli

The MRRs of individual glomeruli in the OB of Rat#2 are listed in Figs. 3 and 4. These figures show that individual glomeruli typically respond to a range of odorants having similar molecular structures. Examination of the relationship between the spatial position and the MRRs of these glomeruli in the first series of experiments (5 rats) clearly indicated that glomeruli with similar MRR tended to gather in close proximity (Figs. 2*J*, 3, and 4). To facilitate the analysis of the spatial representation of the glomerular MRR properties, we tentatively grouped the activated glomeruli into 7 clusters (clusters *A–G*, Fig. 2*J*) based on the similarity of the MRR and the spatial proximity of their position. We further grouped glomeruli within each cluster into several subclusters based on the detailed comparison of molecular structures of effective odorants.

CLUSTER *A*. Glomeruli in the cluster *A* (glom#1–18 in Rat#2) were located at the most anteromedial part of the exposed surface (Fig. 2*J*). Consistent with previous studies (Meister and Bonhoeffer 2001; Uchida et al. 2000), these glomeruli responded to aliphatic acids (red in Fig. 3) and aldehydes (pink). They also responded to a subset of esters (data not shown; cf. Uchida et al. 2000). Glomeruli in the most posterior part of the cluster *A* also responded to diketones (Fig. 3). Thus the characteristic molecular features of odorants effective in activating the cluster *A* glomeruli are a carboxyl group (–COOH), a diketone group [–(CO)(CO)–], or an ester group [–(CO)O–], functional groups having 2 oxygens in a neighborhood. In addition, odorants having a single carbonyl group (–CO) at the end of the molecule were effective in activating the cluster *A* glomeruli.

Molecular features other than the functional groups are also important determinants for the activation of individual glomeruli in the cluster *A*. Based on the carbon chain length of the effective aliphatic acids, we tentatively classified the cluster *A* glomeruli into 3 subclusters: *A-1*, *A-2*, and *A-3* (Figs. 2*J* and 3). Glomeruli in *A-1* responded selectively to aliphatic acids with a long carbon chain (6COOH–8COOH in Fig. 3), those in *A-2* to middle size acids, and those in *A-3* selectively to short aliphatic acids (3COOH–6COOH). A majority of subcluster *A-3* glomeruli also responded to diketones.

CLUSTER *B*. Cluster *B* (glom#20–37 in Rat#2) was located in the most anterior region of the lateral part of the dorsal OB (Fig. 2*J*). Glomeruli in cluster *B* selectively responded to aliphatic alcohols with a long carbon chain (6OH–8OH) and to a wide range of aliphatic ketones (Fig. 3). Additional experiments showed that a majority of cluster *B* glomeruli also responded to anisole derivatives that have a methoxy group (–O–CH_3) and a carbon side chain arranged at the *para*-position of the benzene ring (data not shown; cf. Figs. 5, 6, and 7). Thus the characteristic molecular features of odorants effective in activating the cluster *B* glomeruli are elongated carbon chain structures with a hydroxyl group (–OH), an alkoxyl group (–O–R), or a carbonyl group (–CO) attached at one side of the molecule.

FIG. 2. Relationship between the position of glomeruli and their odorant-response specificity. *A–I*: optical images of intrinsic signals in response to heptanoic acid (*A*), heptanol (*B*), phenol (*C*), *o*-cresol (*D*), phenetole (*E*), butyl ethyl ketone (*F*), menthone (*G*), butyl methyl ether (*H*), and toluene (*I*). Molecular formula of the odorant is shown at the *bottom* of each figure. *A–I* were recorded from the same animal (Rat#1). *J*: spatial position of glomeruli that were activated by at least one of the 72 odorants in the panel. Imaged region covers the dorsal and dorsolateral surfaces of the olfactory bulb (OB) (Rat#2). Glomeruli were numbered from 1 to 119. Glomeruli with similar molecular receptive range (MRR) property were in close proximity and grouped together. MRR of each glomerulus in *J* is shown in Fig. 3 and Fig. 4. Cluster *A* (pink) was located in the most dorsal part of the imaged region. Cluster *B* (yellow and blue), cluster *C* (green), and cluster *D* (blue and pale blue) were arranged from anterior to posterior in the dorsolateral OB. Cluster *E* (white), cluster *F* (blue and gray), and cluster *G* (white and gray) were located in the dorsal part of the lateral surface of the OB. *K*: spatial arrangement of clusters of glomeruli in the dorsal and dorsolateral surfaces of another rat OB (Rat#5). In *J* and *K*, presumable responses of glomeruli near the large blood vessels were not included in the map because of the noises from the vessels. Large indentations of the boundary of the imaged region (thick line), for example, illustrate the position of large vessels. Scale bars: 500 μm.

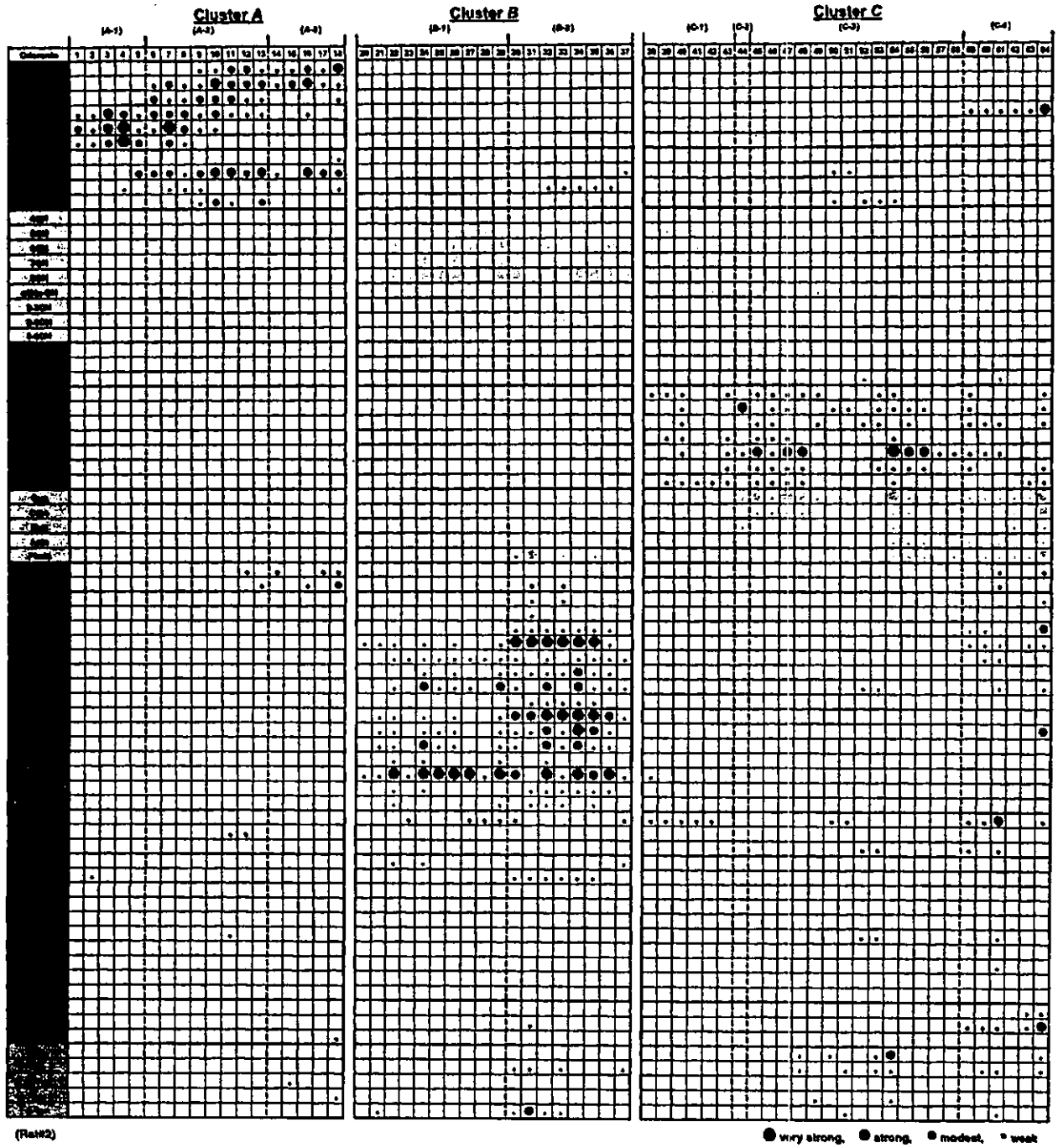

FIG. 3. MRRs of glomeruli within clusters *A*, *B*, and *C*. Glomerular number corresponds to that shown in Fig. 2*J*. *Left column*: stimulus odorants. *Top row*: glomerular number (Rat#2). Cluster *A* was further parceled into 3 subclusters (*A-1* to *A-3*) according to the detailed comparison of their MRR properties. Cluster *B* was further divided into 2 subclusters (*B-1* and *B-2*), cluster *C* into 4 subclusters (*C-1*, *C-2*, *C-3*, and *C-4*). Responses were classified into 4 types: very strong (the largest circle), strong (a large circle), moderate (a small circle), and weak (the smallest circle). Open box indicates no response.

The glomeruli in the posterolateral part of the cluster *B* responded to a wider range of aliphatic ketones and aliphatic alcohols compared with those in the anteromedial part (Figs. 2*J* and 3). We thus tentatively classified cluster *B* glomeruli into 2 subclusters: *B-1* (the anteromedial glomeruli) and *B-2* (the posterolateral glomeruli) (Fig. 2*J*).

CLUSTER *C*. Cluster *C* (glom#38–64 in Rat#2) was located at the central region of the lateral part of the dorsal OB (Fig. 2*J*). Glomeruli in cluster *C* characteristically responded to phenol family odorants (green in Fig. 3; an exception is glom#62). Many of them also responded to phenyl ethers (yellow green). Thus odorants effective in activating cluster *C* glomeruli have

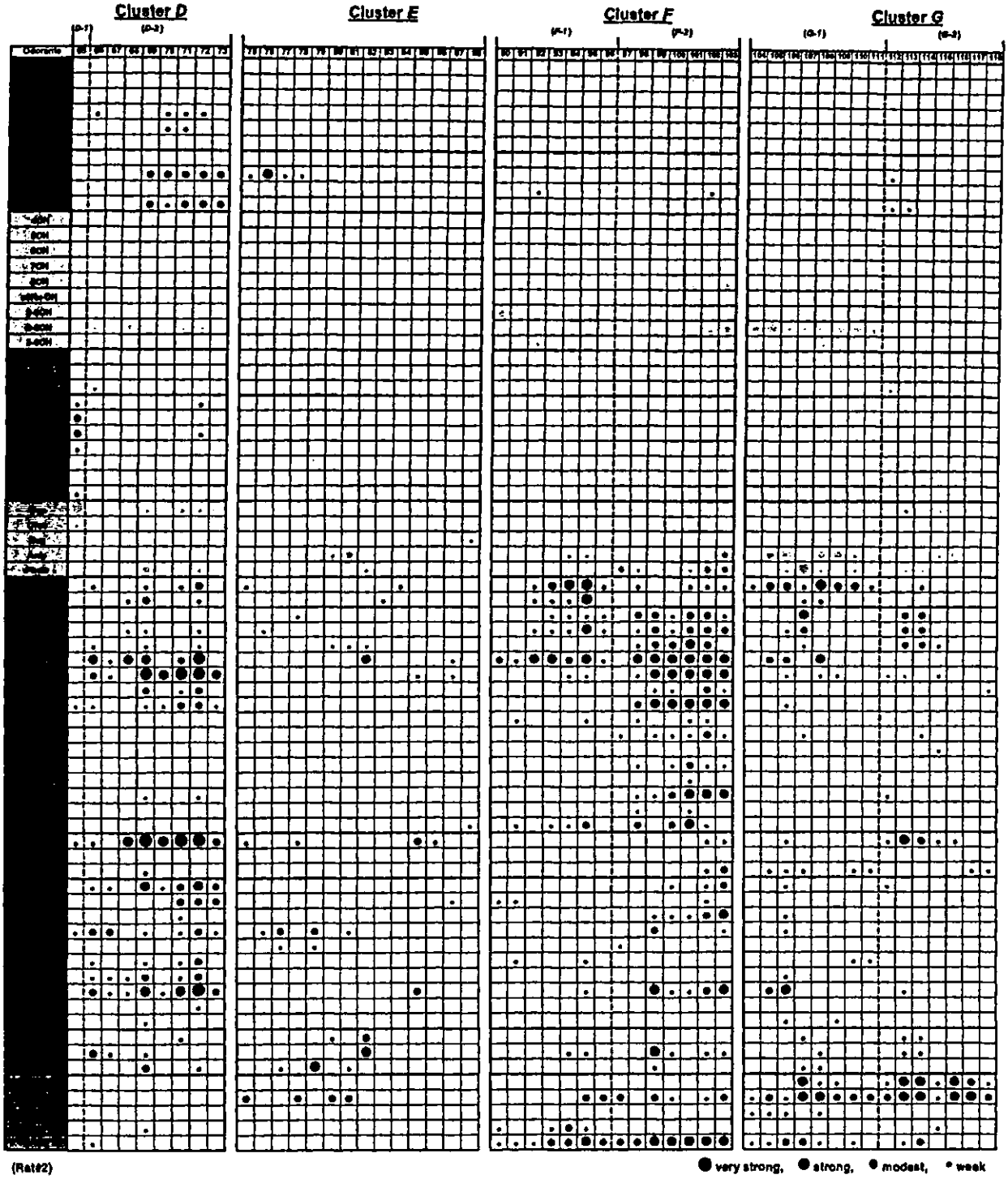

FIG. 4. MRRs of glomeruli within clusters *D*, *E*, *F*, and *G*. Glomerular number corresponds to that shown in Fig. 2*J*. *Left column*: stimulus odorants. *Top row*: glomerular number (Rat#2). Cluster *D* was parceled into 2 subclusters (*D-1* and *D-2*); *F-1* and *F-2*, subclusters in cluster *F*; *G-1* and *G-2*, subclusters in cluster *G*. Responses were classified into 4 types: very strong (the largest circle), strong (a large circle), moderate (a small circle), and weak (the smallest circle). Open box indicates no response.

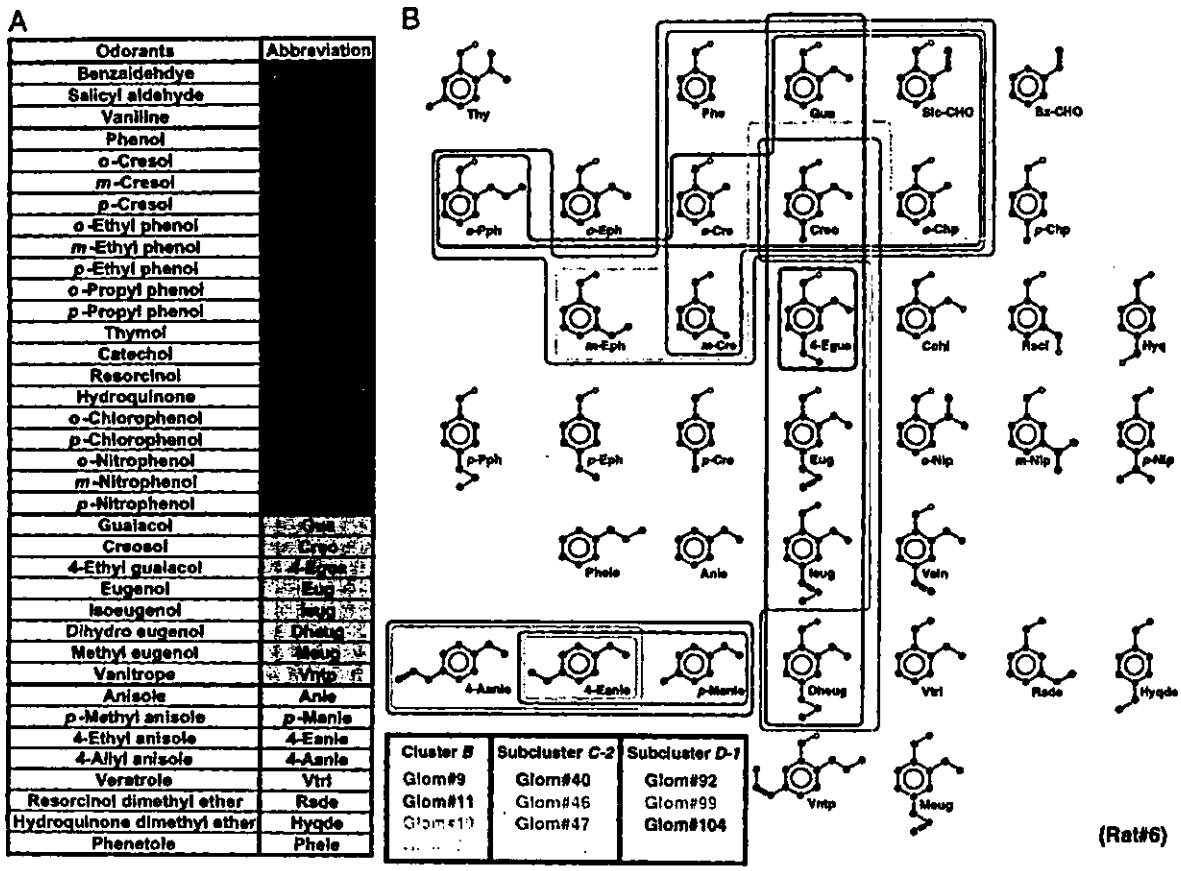

FIG. 5. Panel of aromatic compounds used in the 3rd series of experiments (*A*) and examples of the MRR of individual glomeruli in the panel of aromatic compounds (*B*). Odorants enclosed by each line indicate the MRR of an individual glomerulus. Bluish lines indicate the MRRs of representative glomeruli in cluster *B* (glom#9, #11, #19, and #20) (Rat#6). Reddish lines indicate the MRRs of representative glomeruli within the *C-2* subcluster (glom#40, #46, #47, and #55) (Rat#6). Gray lines indicate the MRRs of representative glomeruli in *D-1* subcluster (glom#92, #99, and #104) (Rat#6). Black dots, red dots, green dots, and blue dots indicate carbon, oxygen, chlorine, and nitrogen atoms, respectively. Hydrogen atom is omitted except for that in the hydroxyl group. Hydrogen atoms are shown by white circles.

a benzene ring with a hydroxyl group, a methoxy group, or an ethoxy group (–O–CH_2–CH_3). Thus the characteristic molecular features include the combination of the benzene ring–like hydrocarbon structure and the functional groups.

Based on the detailed MRR properties and the positions of glomeruli, we tentatively divided the cluster *C* into 4 subclusters: *C-1*, *C-2*, *C-3*, and *C-4* (Fig. 2*J*). In addition to phenol family odorants, *C-1* glomeruli responded to aliphatic alcohols with a relatively short carbon chain (4OH–6OH). *C-2* glomeruli invariably responded to salicyl aldehyde (Slc–CHO in Fig. 5; data not shown), a phenol derivative with a carbonyl group attached to the *ortho*-position. Glomeruli in subcluster *C-3* responded relatively selectively to phenols and phenyl ethers. Glomeruli in subcluster *C-4* also responded to short aliphatic ketones (blue) and aliphatic ethers (purple).

CLUSTER *D*. Cluster *D* glomeruli (glom#65–73 in Rat#2) were located at the caudal region of the lateral part of the dorsal OB (Fig. 2*J*). Although these glomeruli tended to respond to wide structural classes of odorants, odorants effective in activating them were mainly ketones: cyclic ketones, aliphatic–aromatic ketones, diketones, and a subset of aliphatic ketones with relatively short side chains (Fig. 4). Cluster *D* glomeruli were classified into 2 subclusters: medially located *D-1* and laterally located *D-2* (Fig. 2*J*). Many glomeruli in the *D-1* subcluster responded to creosol (Creo in Fig. 1) and eugenol (Eug in Fig. 1; data not shown), phenol derivatives with a methoxy group attached at the *ortho*-position and a carbon side chain at the *para*-position. Because of the presence of a large blood vessel, only one *D-1* glomerulus (glom#65 of Rat#2) was detected in the OB shown in Fig. 2*J*.

Subcluster *D-2* glomeruli tended to respond to aldehydes, alcohols, and ethers in addition to a wide range of ketones. Thus odorants effective in activating the *D-2* glomeruli have a carbonyl group or a hydroxyl group attached to a bulky carbon chain structure.

CLUSTER *E*. Cluster *E* (glom#75–88 in Rat#2) was located at the dorsalmost part of the lateral surface of the OB (Fig. 2*J*). We could not characterize the odorant-response specificity of the cluster *E* glomeruli because they did not respond systematically to any class of the 72 odorants examined (Fig. 4).

CLUSTER *F*. Cluster *F* was located at the rostroventral part of the exposed bulbar surface (Fig. 2*J*). Cluster *F* glomeruli (glom#90–103 in Rat#2) invariably responded to aliphatic ketones and hydrocarbons (Fig. 4). A subset of them also responded to secondary alcohols, phenyl ethers, diketones, and cyclic ketones. Thus odorants effective in activating the cluster *F* glomeruli include not only those with an oxygen-containing group but also hydrocarbon odorants that do not have any polar group. Among the hydrocarbon odorants, cluster *F* glomeruli preferentially responded to terpene hydrocarbons. We tentatively divided cluster *F* glomeruli into 2 subclusters: anteriorly located *F-1* and posteriorly located *F-2* (Fig. 2*J*). Compared with *F-1* glomeruli, those in *F-2* characteristically responded to a wider range of aliphatic and cyclic ketones including terpene ketones. The results suggest that the terpene hydrocarbon structure is one of the main determinants for the activation of *F-2* glomeruli.

CLUSTER *G*. Cluster *G* glomeruli (glom#104–118 in Rat#2) were located at the ventrocaudal part of the imaged region (Fig. 2*J*). Glomeruli in cluster *G* responded to hydrocarbons (Fig. 4). They preferentially responded to benzene family hydrocarbons rather than to terpene hydrocarbons. Many glomeruli in cluster *G* also responded to phenyl ethers, diketones, small aliphatic ketones, aliphatic-aromatic ketones, cyclic ketones, and ethers. Cluster *G* glomeruli were tentatively divided into 2 subclusters: ventrally located *G-1* and dorsally located *G-2* (Fig. 2*J*). *G-1* glomeruli responded to aliphatic alcohols, whereas *G-2* glomeruli did not respond to them.

Using the panel of stimulus odorants in Fig. 1, we examined in detail the MRR properties of clusters *A–D* in 10 rats (first and second series of experiments), and those of clusters *E*, *F*, and *G* in 5 rats (first series of experiment). Figure 2*K* indicates spatial arrangement of the clusters *A–G* in another rat OB (Rat#5). We consistently observed the characteristic odorant-class specificity of each cluster in all the OBs examined. Figure 2, *J* and *K* illustrate an example of interindividual comparison of the spatial arrangement of the clusters *A–G*. Although the shape and the tentative boundary of each cluster varied among different OBs, the glomerular clusters were always located at stereotypical positions and the spatial arrangement of the 7 clusters was conserved in all the OBs examined.

We also noted that some glomeruli at the boundary region between 2 neighboring clusters tended to show MRR properties that are intermediate between those of the 2 clusters. For example, glomeruli #38–43 in cluster *C* responded not only to phenols but also to aliphatic alcohols. In addition, the results in Figs. 3 and 4 suggest that the MRR properties of glomeruli within a given clusters resemble in part those of neighboring glomeruli in adjacent clusters.

A map of characteristic molecular features of odorants

The results shown in Figs. 2, 3, and 4 suggest that ORs represented by glomeruli in a same cluster respond to odorants that have similar molecular features. To examine this possibility, we need to know in detail the characteristic molecular features of odorants that were effective in activating individual glomeruli and to compare the characteristic molecular features among glomeruli in the same cluster and in the neighboring clusters. One possible method to estimate the characteristic molecular features is to characterize and superimpose the 3D structures of odorants effective in activating individual glomeruli. For this purpose, we made a third series of optical imaging experiments (7 rats) using a new panel of odorants that includes a wide variety of aromatic compounds (Fig. 5*A*), the structures of which are semirigid. Because of the limitation of the maximal number of odorants that can be examined in a single rat, however, we omitted many aliphatic compounds, which can have a variety of conformations. Using the new panel of stimulus odorants (see METHODS), we examined in detail the MRR properties of individual glomeruli in clusters *B*, *C*, and *D*.

Figure 5*B* shows examples of the MRR of individual glomeruli in the panel of aromatic compounds. We confirmed that individual glomeruli responded to a range of odorants with similar molecular structure. We also confirmed that glomeruli in a same subcluster showed similar MRR properties. For example, the MRRs of cluster *B* glomeruli (glom#9, #11, #19, and #20 in Rat#6) invariably and selectively covered the series of phenyl ethers that has a carbon chain attached at the *para*-position (surrounded by the bluish lines in Fig. 5*B*). The MRRs of glomeruli in subcluster *C-2* (glom#40, #46, #47, and #55 in Rat#6) always covered a subset of phenols, a subset of methoxyphenols, and salicyl aldehyde (Slc–CHO) (surrounded by the reddish lines in Fig. 5*B*). The MRRs of subcluster *D-1* glomeruli (glom#92, #99, and #104 in Rat#6) invariably covered eugenol family odorants (surrounded by the gray lines in Fig. 5*B*).

The characteristic molecular features of individual glomeruli were estimated by superimposing the 3D structure of the effective aromatic compounds. For example, glomerulus #46 in subcluster *C-2* of Rat#6 responded strongly to guaiacol (Gua) and salicyl aldehyde (Slc–CHO); moderately to phenol (Phe), *o*-cresol (*o*-Cre), and *o*-chlorophenol (*o*-Chp); and weakly to *m*-cresol (*m*-Cre) and creosol (Creo) (Fig. 6*A*). Because these compounds have semirigid structures, the most stable conformations of the compounds were used for the molecular superposition. The superposition of the 3D structures of the compounds was performed by least-square fitting using the atoms numbered 1–7 in Fig. 6*A*. Superimposed 3D structures are shown in Fig. 6*B*. A total van der Waals (VDW) volume of the superimposed structures is also shown in Fig. 6*C*. It is likely that the superimposed 3D structures and their VDW volume give the information about the shape and physicochemical properties of the characteristic molecular features of the effective odorants. To make it clear, a 2D representation of the VDW volume is shown in Fig. 6*D*.

Figure 6, *E–H* show another example of the molecular superimposition. This glomerulus (#4 in cluster *B* of Rat#6) responded weakly to 4-ethyl anisole (4-Eanle) and 4-allyl anisole (4-Aanle). In addition, it responded to aliphatic compounds, octyl alcohol (8OH), butyl methyl ketone (K4-1), pentyl ethyl ketone (K5-2), hexyl methyl ketone (K6-1), and heptyl propyl ketone (K7-3). The characteristic molecular features were estimated based on the conformations of the 3D structure of the 2 aromatic compounds (4-Eanle and 4-Aanle). Then, to ascertain whether the 3D structures of the aliphatic compounds overlap well with the aromatic compounds, a set of energy-minimized conformers for each aliphatic compound was calculated and was superimposed on 4-ethyl anisole used

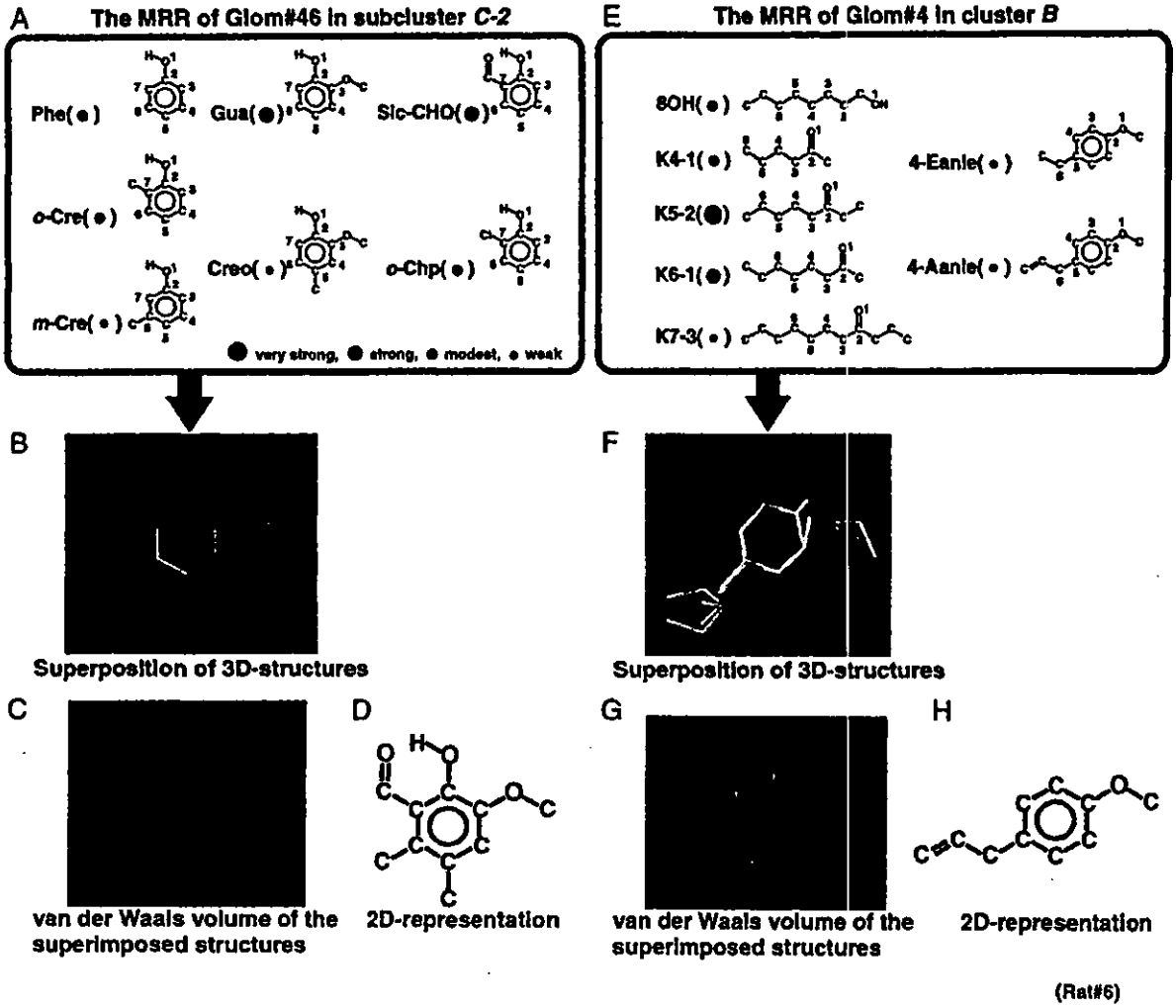

FIG. 6. Schematic diagrams illustrating the method for the superimposition of the 3D structures of the odorants effective in activating individual glomeruli. *A* and *E*: abbreviated name and molecular formula of odorants that activated glom#46 in subcluster *C-2* (*A*) or glom#4 in cluster *B* (*E*) of Rat#6, respectively. Magnitude of the glomerular response to each odorant is shown by symbols: the largest circle (very strong), a large circle (strong), a small circle (moderate), and the smallest circle (weak). Superposition of the 3D structures of the compounds was performed by least-square fitting using the atoms, numbered 1–7 in *A* or 1–6 in *E*, respectively. Superimposed 3D structures are shown in *B* and *F*. A total van der Waals (VDW) volume or the superimposed structures is shown in *C* and *G*. 2D representation of the VDW volume is shown in *D* and *H*.

as a template molecule. As shown in Fig. 6*F*, a conformer that overlaps well could be extracted for each aliphatic compound. A total VDW volume of the superimposed structures and its 2D representation are also shown in Fig. 6, *G* and *H*, respectively. A similar superposition based on the 3D structures of the effective odorants was carried out for the other glomeruli.

Figure 7 shows a map of the 2D structures of the characteristic molecular features in the OB of a rat (Rat#6). To facilitate the analysis, we labeled the presumed critical parts of the characteristic molecular features. The molecular features composed of a single methoxy or a single ethoxy group are indicated by blue shadows, those of a single hydroxyl group by yellow shadows. The molecular features that were composed of a combination of a single hydroxyl group and a single alkoxyl group arranged at the *ortho*-position are indicated by red surroundings, and those of a single hydroxyl group and a single carbonyl group arranged at the *ortho*-position by pink surroundings.

Interestingly, the map of characteristic molecular features (Fig. 7) showed a systematic and gradual change in the features according to the position of subclusters along the OB axes. For example, subcluster *C-2* glomeruli typically responded to salicyl aldehyde (Slc–CHO in Fig. 5) that has a hydroxyl group and an aldehyde group (–CHO) arranged at the *ortho*-position (indicated by pink surroundings in Fig. 7). The characteristic molecular features of glomeruli in the *C-2* subcluster thus include 2 oxygens in a neighborhood. Because the glomeruli in cluster *A* (glom#12, #51–53, #65, and #76) can respond to aliphatic acids, diketones, and esters that have 2 oxygens in a neighborhood, the results suggest that the characteristic mo-

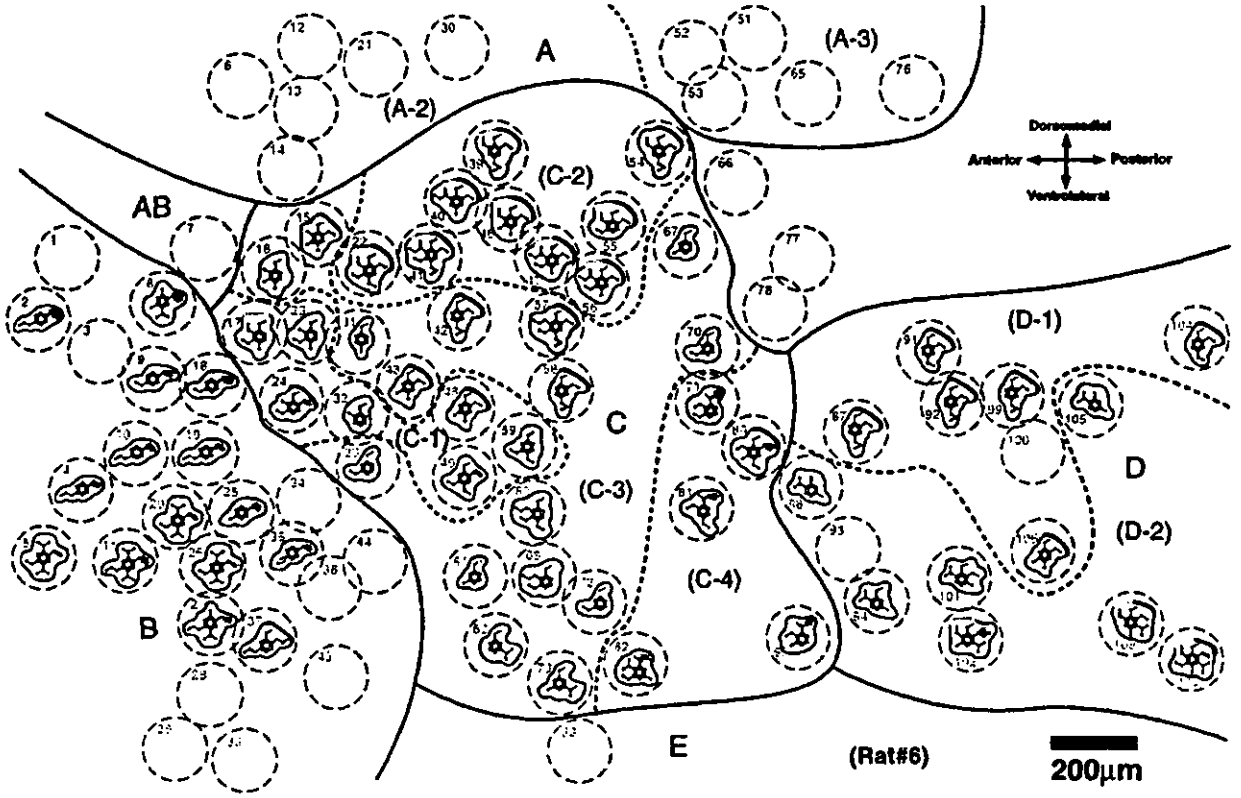

FIG. 7. Map of the characteristic molecular features. Positions of individual glomeruli are shown by gray interrupted circles with glomerular number (of Rat#6). Presumed critical parts of the characteristic molecular features are labeled by colors. Blue shadows indicate the molecular features composed of a methoxy or an ethoxy group. If a glomerulus responded to a benzene derivative with only a single methoxy or a single ethoxy group, the group was shadowed by blue. Yellow shadows indicate the molecular features that are composed of a single hydroxyl group. Red surroundings indicate the molecular features composed of a combination of a hydroxyl group and an alkoxyl group arranged at *ortho*-position. Pink surroundings indicate the molecular features composed of a combination of a hydroxyl group and a carbonyl group arranged at the *ortho*-position. Scale bar: 200 μm.

lecular features of *C-2* glomeruli partially resemble those of neighboring cluster *A* glomeruli.

When we consider overall molecular structure and the functional groups, salicyl aldehyde closely resembles benzoic acid and benzaldehyde (Bz–CHO in Fig. 5). In accord with this, additional experiments showed that benzoic acid and benzaldehyde activated several glomeruli in subclusters *A-2* and *A-3* (glom#12, #21, #30, and #51–53 in Fig. 7) that directly appose to subcluster *C-2*. This suggests that characteristic molecular features of the *C-2* subcluster closely resemble those of the *A-2* and *A-3* subclusters.

Subcluster *C-2* glomeruli also responded to methoxyphenols (indicated by red surroundings in Fig. 7) that have a hydroxyl group and a methoxy group arranged at the *ortho*-position around a benzene ring. The area occupied by the methoxyphenol-responsive glomeruli extended anterolaterally from subcluster *C-2* to the medial part of subcluster *C-3* and even to a part of subcluster *C-1*. This suggests that the subset of methoxyphenol-responsive glomeruli resembles each other in terms of the characteristic molecular features of the effective odorants.

Subcluster *C-1* glomeruli characteristically responded to short aliphatic alcohols (4OH–6OH) in addition to phenols. A few *C-1* glomeruli also responded to phenyl ethers having a methoxy group and a carbon side chain attached at the *para*-position (shown by blue shadows, glom#24 and #49 in Fig. 7). The glomeruli in the neighboring cluster *B* invariably responded to long aliphatic alcohols (6OH–8OH) and a majority of them also responded to phenyl ethers with a carbon chain attached at the *para*-position (blue shadows, glom#2, #4, #5, #8–11, #18–20, #25–27, and #35 in Fig. 7). The observation suggests that the characteristic molecular features of *C-1* glomeruli partially resemble those of the neighboring cluster *B*.

Thus by the stepwise comparison of the characteristic molecular features of glomeruli in the chains of subclusters *A-2*, *C-2*, the medial part of *C-3*, *C-1*, and cluster *B*, we noted a systematic and gradual change in the characteristic molecular features. Another example is the characteristic molecular features of glomeruli in the neighboring subclusters *C-4*, *D-1*, and *D-2*. Glomeruli in subcluster *C-4* characteristically responded to aliphatic and cyclic ketones in addition to phenols. Glomeruli in subcluster *D-2* typically responded to the aliphatic and cyclic ketones, suggesting the similarity in the characteristic molecular features between the 2 neighboring subclusters.

The *C-4* subcluster characteristically responded to phenols with a hydroxyl group and phenyl ethers with a methoxy group. The glomeruli in subcluster *D-1* characteristically re-

sponded to eugenol family odorants, methoxyphenols that have a hydroxyl group and a methoxy group. This suggests that the characteristic molecular features of *D-1* glomeruli partially resemble those of *C-4* glomeruli.

Thus the similarity in the characteristic molecular features was noted not only between 2 neighboring subclusters in a same cluster but also between 2 neighboring subclusters each belonging to a different cluster. We also noted that clusters *A–D* partially overlapped and were not completely segregated from each other. For example, we observed in many OBs that cluster *A* partially overlapped with cluster *B* so that a few glomeruli in the overlapped part responded to aliphatic acids and aliphatic alcohols (shown by *AB* in Figs. 2*K* and 7). These results suggest a gradual change in the characteristic molecular features according to the position of glomeruli within clusters *A–D*.

Bulbar zones and clusters

Glomeruli in the OB can be classified into zonal subsets (Mori and Yoshihara 1995; Mori et al. 1999; Schwob et al. 1986). To examine the spatial arrangement of clusters *A–G* relative to the bulbar zones, we dye-marked several points after the optical imaging of these clusters in 3 rats. The sections of the OB containing the marked points were labeled by anti-OCAM antibody to distinguish glomeruli in zone 1 (OCAM-negative) and those in zones 2–4 (OCAM-positive) (Fig. 8, *A* and *B*) (Yoshihara et al. 1997). From a series of the labeled sections, we made a flattened unrolled map of glomeruli (Nagao et al. 2000). Based on the positions of the dye-marked points, we then superimposed clusters *A–G* on the flattened glomerular map (Fig. 8*C*). The results showed that most glomeruli in clusters *A–D* were in the OCAM-negative zone 1, whereas those in clusters *F* and *G* were in the OCAM-positive zones 2–4. The boundary line between OCAM-negative and OCAM-positive zones was located near the lateral margin of clusters *B*, *C*, and *D* and presumably in cluster *E*. In a clear correspondence with the zonal classification of the clusters, clusters *A–D* glomeruli in zone 1 responded to odorants with polar functional group(s), whereas clusters *F* and *G* glomeruli (in zones 2–4) can respond to hydrocarbon odorants in addition to those having polar group(s).

DISCUSSION

Glomerular clusters and subclusters

Present results indicate that similar characteristic molecular features map to neighboring glomeruli (Fig. 7). Thus one of the distinct properties of the OR map is the local clustering of glomeruli that represent similar characteristic molecular features. Such clustering of glomeruli is not evident in the anten-

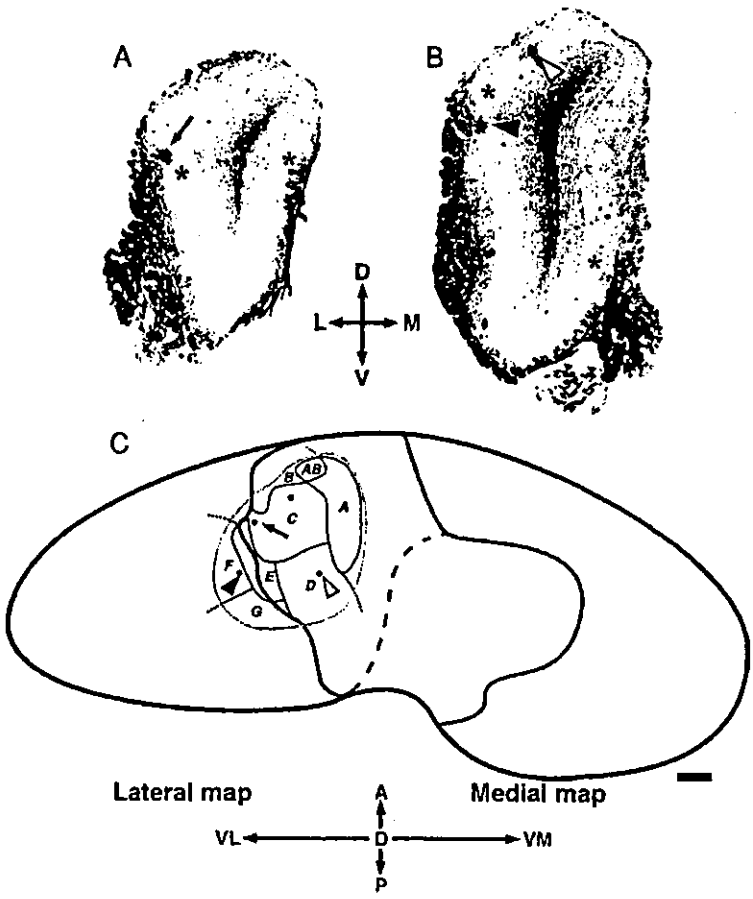

FIG. 8. Position of clusters *A–G* in the flattened unrolled map of glomeruli in the OB. *A* and *B*: coronal sections of the OB labeled with anti- olfactory cell adhesion molecule (OCAM) antibody (black). Boundaries between OCAM-positive and -negative zones are indicated with asterisks. Black arrow, black arrowhead, and white arrowhead indicate dye-marked points. *C*: unrolled map of the glomerular layer of the OB. OCAM-positive zones (zones 2–4) are indicated by gray shading. White area indicates OCAM-negative zone (zone 1). Thick dotted line indicates presumed boundary between the medial map and the lateral map. Imaged region is shown by gray line. Black dots indicate dye-marked points. Black arrow, black arrowhead, and white arrowhead correspond to the dye-marked points shown in *A* and *B*. Positions of clusters *A–G* are indicated by characters *A–G*, respectively. A, anterior; D, dorsal; L, lateral; M, medial; VL, ventrolateral; VM, ventromedial. Scale bar: 500 μm.

nal lobe of the fly brain (Wang et al. 2003), and thus may be the characteristic of the vertebrate OB. In the present study, we tentatively classified 7 clusters and 15 subclusters of glomeruli in the dorsal and dorsolateral surfaces of the OB. Because ORs having similar MRR properties may be highly homologous in amino acid sequence, the clustering of glomeruli with similar MRRs in the map is in good agreement with previous reports that olfactory sensory neurons expressing highly related ORs appear to project their axons to glomeruli that are in close proximity (Strotmann et al. 2000; Tsuboi et al. 1999).

Based on the amino acid sequences, numerous types of mouse ORs are classified into 228 families (Zhang and Firestein 2002). This raises a possibility that ORs represented in a same cluster or a same subcluster might belong to a specific OR family or a combination of OR families, which were presumably evolved by gene duplication and gene mutation. The clustering of glomeruli representing like ORs suggests that the gene duplication involves both the OR gene and the loci controlling the olfactory axon projection to the target glomeruli.

The imaged region covers a large part of the OCAM-negative zone (zone 1) and a small part of OCAM-positive zones (zones 2–4) of the lateral map (Fig. 8). Except for the characterless cluster *E*, the imaged region is covered by the clusters and subclusters that can be defined by the characteristic molecular features of effective odorants. Glomerular clusters with similar MRR properties are also present in the lateral and lateroventral surfaces of the OB (K. Igarashi and K. Mori, unpublished observations). These results suggest that the clustering of glomeruli having similar MRRs is present throughout the OR map, and is one of the basic plans for the spatial arrangement of glomeruli. The clustering of glomeruli handling similar but slightly different molecular structures may help to sharpen the discrimination of subtle difference in odorant structure (Imamura et al. 1992; Katoh et al. 1993; Mori et al. 1999; Yokoi et al. 1995).

The clusters and subclusters classified thus far were stereotypically arranged in the glomerular sheet and were conserved among different rats. Odorants that activate glomeruli in a specific cluster or subcluster in the rat OB tend to contain similar "odor " to human nose. For example, the anisole family odorants (Anle, *p*-Manle, 4-Eanle, and 4-Aanle in Fig. 5) that activate glomeruli in cluster *B* have an "aniseed odor " in common. Cluster *C* glomeruli were activated by phenols, which have a "phenolic odor. " Salicyl aldehyde, benzaldehyde, and benzoic acid activate glomeruli in subcluster *C-2* and neighboring subcluster *A-2*. These odorants have an "almond-like odor. " Eugenol family odorants (Gua, Creo, 4-Egua, Eug, Ieug, and Dheug in Fig. 5) activated glomeruli in the medial part of cluster *C* and in subcluster *D-1*. These odorants contain a "clove oil odor " in common. We previously noted the correlation of the glomeruli in cluster *A* to the "pungent, sour, fatty, and rancid odor " (Uchida et al. 2000). These results thus corroborate the hypothesis that the clustering of glomeruli having similar MRRs might participate in the neuronal mechanisms responsive for odor quality perception. The map of the characteristic molecular features might provide the neuronal basis for the relationship between the odorant molecular structure and the subjectively perceived "odor quality " (Moncrieff 1967).

Topographical map of the characteristic molecular features

By superimposing the 3D structures of effective aromatic compounds, we deduced the characteristic molecular features of glomeruli in cluster *C* and neighboring subclusters. Although the estimation of the characteristic molecular features is incomplete and the range of subclusters explored with this method were very limited, the map (Fig. 7) showed a systematic and gradual change in the characteristic molecular features according to the position of subclusters along the axes in zone 1 of the lateral map. This suggests the presence of the topographic map of the characteristic molecular features in zone 1 of the OB.

Although we tentatively grouped glomeruli into clusters and subclusters, the continual representation of the characteristic molecular features suggests that the glomerular map is not composed of mosaics of discrete clusters (and subclusters), each with completely different characteristic molecular features. Instead, 2 neighboring clusters show similarity in the characteristic molecular features, and in many cases partially overlap each other. Two neighboring subclusters, either in a same cluster or each in a different cluster, typically show similar characteristic molecular features. We propose that the glomerular map in zone 1 represents the characteristic molecular features in a systematic and continual way such that the characteristic molecular features gradually change along the axes in the map. We thus used the term "clusters" instead of the previously used term "domains" (Uchida et al. 2000).

ORs are 7-transmembrane G protein–coupled receptors (Buck and Axel 1991). Knowledge of the 3D structure of other G protein–coupled receptors such as rhodopsin (Okada et al. 2002; Palczewski et al. 2000) suggests that each OR might have a specific ligand-binding-site (odorant-receptive-site) structure formed by the bundle of transmembrane segments (Singer et al. 1995; Vaidehi et al. 2002). The distinct odorant-receptive-site structure of each OR might determine the odorant-response specificity of the OR. If this is the case and if the characteristic molecular features of individual glomeruli strongly reflect the odorant-response specificity of the represented ORs, present results imply that odorant-receptive-site structures of ORs might be gradually and systematically represented in the glomerular sensory map of the OB.

Previous and present studies of activity mapping showed that carbon chain length of aliphatic acids and aldehydes was systematically represented with a gradual shift of the position of activated glomeruli within cluster *A* (Inaki et al. 2002; Johnson et al. 1999; Meister and Bonhoeffer 2001; Rubin and Katz 1999; Uchida et al. 2000). From short to long, the chain length is represented by overlapping glomeruli whose position shifts gradually from subcluster *A-3* through subclusters *A-2* to *A-1*. Similarly, the chain length of aliphatic alcohols was represented by overlapping glomeruli whose position shifts from subcluster *C-1* to cluster *B*. The systematic representation of the carbon chain length thus reflects the gradual change in the characteristic molecular features along consecutive series of subclusters in the OR map.

The systematic and continual representation of stimulus or receptor attributes is a common feature of mammalian primary sensory cortices. However, the map of the characteristic molecular features in the OB is unique among sensory maps in the brain. The presence of nearly 1,000 types of ORs might

necessitate the central olfactory system to map the numerous characteristic molecular features of odorants to a large space of the glomerular sheet.

What is the functional significance of the systematic spatial map of the characteristic molecular features? Mitral cells in the OB read the glomerular map and then send their output to the olfactory cortex (Shepherd and Greer 1998). Individual mitral cells project a single primary dendrite to a single glomerulus and receive olfactory axon input within the glomerulus. In addition, individual mitral cells emit several secondary dendrites tangentially and receive inhibitory inputs by local interneurons from neighboring mitral cells that innervate neighboring glomeruli. Thus the output of a mitral cell is the consequence of the integration of the direct input from its own glomerulus and the indirect inputs from many neighboring glomeruli. Because individual mitral cells emit long (~1 mm) secondary dendrites to a variety of directions (Orona et al. 1984), a mitral cell may integrate signals not only from glomeruli in the same subcluster and the same cluster, but also from those in neighboring clusters. In accordance with this, we observed that the activities of mitral cells are strongly influenced by the odorants that activated neighboring glomeruli (Nagayama et al. 2004). The integration of signals from its own glomerulus and surrounding glomeruli seems to be especially important for the processing of signals evoked by a complex mixture of odorants that occur in the natural environment. Spatial arrangement of the OR-representing glomeruli is thus a key factor to the manner of the olfactory signal processing in the neuronal circuit of the OB.

ACKNOWLEDGMENTS

We thank Dr. Yoshihara and members of the Department of Physiology for comments on the manuscript.

GRANTS

This work was supported by Grants-in-aids for Creative Scientific Research (K. Mori) and for Young Scientists (Y. K. Takahashi) from Japan Society for the Promotion of Science.

REFERENCES

Belluscio L and Katz LC. Symmetry, stereotypy, and topography of odorant representations in mouse olfactory bulbs. *J Neurosci* 21: 2113–2122, 2001.

Buck L and Axel R. A novel multigene family may encode odorant receptors: a molecular basis for odor recognition. *Cell* 65: 175–187, 1991.

Coopersmith R, Henderson SR, and Leon M. Odor specificity of the enhanced neural response following early odor experience in rats. *Brain Res* 392: 191–197, 1986.

Fried HU, Fuss SH, and Korsching SI. Selective imaging of presynaptic activity in the mouse olfactory bulb shows concentration and structure dependence of odor responses in identified glomeruli. *Proc Natl Acad Sci USA* 99: 3222–3227, 2002.

Imamura K, Mataga N, and Mori K. Coding of odor molecules by mitral/tufted cells in rabbit olfactory bulb. I. Aliphatic compounds. *J Neurophysiol* 68: 1986–2002, 1992.

Inaki K, Takahashi YK, Nagayama S, and Mori K. Molecular-feature domains with posterodorsal-anteroventral polarity in the symmetrical sensory maps of the mouse olfactory bulb: mapping of odourant-induced Zif268 expression. *Eur J Neurosci* 15: 1563–1574, 2002.

Johnson BA, Woo CC, Hingco EE, Pham KL, and Leon M. Multidimensional chemotopic responses to n-aliphatic acid odorants in the rat olfactory bulb. *J Comp Neurol* 409: 529–548, 1999.

Johnson BA, Woo CC, and Leon M. Spatial coding of odorant features in the glomerular layer of the rat olfactory bulb. *J Comp Neurol* 393: 457–471, 1998.

Katoh K, Koshimoto H, Tani A, and Mori K. Coding of odor molecules by mitral/tufted cells in rabbit olfactory bulb. II. Aromatic compounds. *J Neurophysiol* 70: 2161–2175, 1993.

Leon M and Johnson BA. Olfactory coding in the mammalian olfactory bulb. *Brain Res Brain Res Rev* 42: 23–32, 2003.

Meister M and Bonhoeffer T. Tuning and topography in an odor map on the rat olfactory bulb. *J Neurosci* 21: 1351–1360, 2001.

Mombaerts P, Wang F, Dulac C, Chao SK, Nemes A, Mendelsohn M, Edmondson J, and Axel R. Visualizing an olfactory sensory map. *Cell* 87: 675–686, 1996.

Moncrieff RW. *The Chemical Senses.* London: Leonard Hill, 1967.

Mori K, Nagao H, and Yoshihara Y. The olfactory bulb: coding and processing of odor molecule information. *Science* 286: 711–715, 1999.

Mori K and Yoshihara Y. Molecular recognition and olfactory processing in the mammalian olfactory system. *Prog Neurobiol* 45: 585–619, 1995.

Nagao H, Yoshihara Y, Mitsui S, Fujisawa H, and Mori K. Two mirror-image sensory maps with domain organization in the mouse main olfactory bulb. *Neuroreport* 11: 3023–3027, 2000.

Nagayama S, Takahashi YK, Yoshihara Y, and Mori K. Mitral and tufted cells differ in the decoding manner of odor maps in the rat olfactory bulb. *J Neurophysiol* 91: 2532–2540, 2004.

Okada T, Fujiyoshi Y, Silow M, Navarro J, Landau EM, and Shichida Y. Functional role of internal water molecules in rhodopsin revealed by X-ray crystallography. *Proc Natl Acad Sci USA* 99: 5982–5987, 2002.

Orona E, Rainer EC, and Scott JW. Dendritic and axonal organization of mitral and tufted cells in the rat olfactory bulb. *J Comp Neurol* 226: 346–356, 1984.

Palczewski K, Kumasaka T, Hori T, Behnke CA, Motoshima H, Fox BA, Le Trong I, Teller DC, Okada T, Stenkamp RE, Yamamoto M, and Miyano M. Crystal structure of rhodopsin: a G protein-coupled receptor. *Science* 289: 739–745, 2000.

Ressler KJ, Sullivan SL, and Buck LB. Information coding in the olfactory system: evidence for a stereotyped and highly organized epitope map in the olfactory bulb. *Cell* 79: 1245–1255, 1994.

Royet JP, Sicard G, Souchier C, and Jourdan F. Specificity of spatial patterns of glomerular activation in the mouse olfactory bulb: computer-assisted image analysis of 2-deoxyglucose autoradiograms. *Brain Res* 417: 1–11, 1987.

Rubin BD and Katz LC. Optical imaging of odorant representations in the mammalian olfactory bulb. *Neuron* 23: 499–511, 1999.

Schwob JE and Gottlieb DI. The primary olfactory projection has two chemically distinct zones. *J Neurosci* 6: 3393–3404, 1986.

Shepherd GM and Greer CA. Olfactory bulb. In: *The Synaptic Organization of the Brain* (4th ed.), edited by Shepherd GM. New York: Oxford Univ. Press, 1998, p. 159–203.

Singer MS, Oliveira L, Vriend G, and Shepherd GM. Potential ligand-binding residues in rat olfactory receptors identified by correlated mutation analysis. *Receptors Channels* 3: 89–95, 1995.

Spors H and Grinvald A. Spatio-temporal dynamics of odor representations in the mammalian olfactory bulb. *Neuron* 34: 301–315, 2002.

Stewart WB, Kauer JS, and Shepherd GM. Functional organization of rat olfactory bulb analysed by the 2-deoxyglucose method. *J Comp Neurol* 185: 715–734, 1979.

Strotmann J, Conzelmann S, Beck A, Feinstein P, Breer H, and Mombaerts P. Local permutations in the glomerular array of the mouse olfactory bulb. *J Neurosci* 20: 6927–6938, 2000.

Tsuboi A, Yoshihara S, Yamazaki N, Kasai H, Asai-Tsuboi H, Komatsu M, Serizawa S, Ishii T, Matsuda Y, Nagawa F, and Sakano H. Olfactory neurons expressing closely linked and homologous odorant receptor genes tend to project their axons to neighboring glomeruli on the olfactory bulb. *J Neurosci* 19: 8409–8418, 1999.

Uchida N, Takahashi YK, Tanifuji M, and Mori K. Odor maps in the mammalian olfactory bulb: domain organization and odorant structural features. *Nat Neurosci* 3: 1035–1043, 2000.

Vaidehi N, Floriano WB, Trabanino R, Hall SE, Freddolino P, Choi EJ, Zamanakos G, and Goddard WA 3rd. Prediction of structure and function of G protein-coupled receptors. *Proc Natl Acad Sci USA* 99: 12622–12627, 2002.

Vassar R, Chao SK, Sitcheran R, Nunez JM, Vosshall LB, and Axel R. Topographic organization of sensory projections to the olfactory bulb. *Cell* 79: 981–991, 1994.

Wachowiak M and Cohen LB. Representation of odorants by receptor neuron input to the mouse olfactory bulb. *Neuron* 32: 723–735, 2001.

Wang JW, Wong AM, Flores J, Vosshall LB, and Axel R. Two-photon calcium imaging reveals an odor-evoked map of activity in the fly brain. *Cell* 112: 271–282, 2003.

Xu F, Liu N, Kida I, Rothman DL, Hyder F, and Shepherd GM. Odor maps of aldehydes and esters revealed by functional MRI in the glomerular layer of the mouse olfactory bulb. *Proc Natl Acad Sci USA* 100: 11029–11034, 2003.

Yang X, Renken R, Hyder F, Siddeek M, Greer CA, Shepherd GM, and Shulman RG. Dynamic mapping at the laminar level of odor-elicited responses in rat olfactory bulb by functional MRI. *Proc Natl Acad Sci USA* 95: 7715–7720, 1998.

Yokoi M, Mori K, and Nakanishi S. Refinement of odor molecule tuning by dendrodendritic synaptic inhibition in the olfactory bulb. *Proc Natl Acad Sci USA* 92: 3371–3375, 1995.

Yoshihara Y, Katoh K, and Mori K. Odor stimulation causes disappearance of R4B12 epitope on axonal surface molecule of olfactory sensory neurons. *Neuroscience* 53: 101–110, 1993.

Yoshihara Y, Kawasaki M, Tamada A, Fujita H, Hayashi H, Kagamiyama H, and Mori K. OCAM: a new member of the neural cell adhesion molecule family related to zone-to-zone projection of olfactory and vomeronasal axons. *J Neurosci* 17: 5830–5842, 1997.

Zhang X and Firestein S. The olfactory receptor gene superfamily of the mouse. *Nat Neurosci* 5: 124–133, 2002.

Design, Synthesis, and Biological Evaluation of New Cyclic Disulfide Decapeptides That Inhibit the Binding of AP-1 to DNA

Keiichi Tsuchida, Hisaaki Chaki, Tadakazu Takakura, Junichi Yokotani, Yukihiko Aikawa, Shunichi Shiozawa, Hiroaki Gouda, and Shuichi Hirono

Discovery Laboratories and Research Laboratories, Toyama Chemical Co., Ltd., 4-1 Shimookui 2-chome, Toyama 930-8508, Japan, Department of Rheumatology, Faculty of Health Science, Kobe University School of Medicine, 7-10-2 Tomogaoka, Suma-ku, Kobe 654-0142, Japan, Rheumatic Disease Division, Kobe University Hospital, 7-5-2 Kusunoki-cho, Chuo-ku, Kobe 650-0017, Japan, and School of Pharmaceutical Sciences, Kitasato University, 5-9-1 Shirokane, Minato-ku, Tokyo 108-8641, Japan

JOURNAL OF
MEDICINAL CHEMISTRY®

Reprinted from
Volume 47, Number 17, Pages 4239–4246

Design, Synthesis, and Biological Evaluation of New Cyclic Disulfide Decapeptides That Inhibit the Binding of AP-1 to DNA

Keiichi Tsuchida,*,† Hisaaki Chaki,‡ Tadakazu Takakura,† Junichi Yokotani,† Yukihiko Aikawa,‡ Shunichi Shiozawa,§,∥ Hiroaki Gouda,⊥ and Shuichi Hirono⊥

Discovery Laboratories and Research Laboratories, Toyama Chemical Co., Ltd., 4-1 Shimookui 2-chome, Toyama 930-8508, Japan, Department of Rheumatology, Faculty of Health Science, Kobe University School of Medicine, 7-10-2 Tomogaoka, Suma-ku, Kobe 654-0142, Japan, Rheumatic Disease Division, Kobe University Hospital, 7-5-2 Kusunoki-cho, Chuo-ku, Kobe 650-0017, Japan, and School of Pharmaceutical Sciences, Kitasato University, 5-9-1 Shirokane, Minato-ku, Tokyo 108-8641, Japan

Received February 4, 2004

The transcription factor activator protein-1 (AP-1) is an attractive target for the treatment of immunoinflammatory diseases, such as rheumatoid arthritis. Using the three-dimensional (3D) X-ray crystallographic structure of the DNA-bound basic region leucine zipper (bZIP) domains of AP-1, new cyclic disulfide decapeptides were designed and synthesized that demonstrated AP-1 inhibitory activities. The most potent inhibition was exhibited by Ac-c[Cys-Gly-Gln-Leu-Asp-Leu-Ala-Asp-Gly-Cys]-NH_2 (peptide **2**) (IC_{50} = 8 μM), which was largely due to the side chains of residues 3–6 and 8 of the peptide, as shown by an alanine scan. To provide structural information about the biologically active conformation of peptide **2**, the structures of peptide **2** derived from molecular dynamics simulation of the bZIP–peptide **2** complex with explicit water molecules were superimposed on the solution structures derived from NMR measurements of peptide **2** in water. These showed a strong structural similarity in the backbones of residues 3–7 and enabled the construction of a 3D pharmacophore model of AP-1 binding compounds, based on the chemical and structural features of the amino acid side chains of residues 3–7 in peptide **2**.

Introduction

Activator protein-1 (AP-1) is an important transcription factor for genes involved in immune and inflammatory responses, such as cytokines and collagenase.[1-3] Various inflammatory and mitogenic stimulations lead to AP-1 activation, and it probably plays a role in rheumatoid arthritis, transplant rejection, and tumor growth, so it is an attractive therapeutic target for the treatment of such disorders.[4] Indeed, systematic administration of an AP-1 decoy oligodeoxynucleotide containing the AP-1 binding site was found to inhibit arthritic joint destruction in mice with collagen-induced arthritis.[5] AP-1 is composed of members of the Fos and Jun families.[1] Fos and Jun proteins dimerize through a leucine zipper motif at their carboxyl terminals and bind DNA through a basic region that is located immediately upstream of the leucine zipper.[1,6] The three-dimensional (3D) X-ray crystallographic structure[7] of the basic region leucine zipper (bZIP) domains of c-Fos and c-Jun bound to a 20 nucleotide DNA duplex containing the AP-1 binding site revealed single α-helices and showed that the heterodimer grips the major groove of the DNA like a pair of forceps. Although the solution structure of the bZIP domains of AP-1 in the absence of DNA is unclear, the effect of dimerization and DNA binding on circular dichroism (CD) spectra of the bZIP domains suggested that the basic regions of the domains take on an α-helical conformation only in the presence of DNA.[8] In support of this, the solution structure of the yeast transcriptional factor GCN4 bZIP domain, as determined by NMR, revealed that the leucine zipper region forms a long uninterrupted α-helix and the basic region is flexible but structured, fluctuating around a helical conformation in the absence of DNA.[9]

Structure-based drug design methods have strongly enhanced the lead discovery and optimization process using the 3D structures of target proteins, which are important for understanding the interaction between the ligand and the target protein.[10,11] Recently, natural products such as curcumin,[12,13] dihydroguaiaretic acid,[12,14] momordin,[15] and a new anthraquinone derivative[16] were reported to inhibit the binding of AP-1 to the AP-1 binding site. However, 3D structural information about the AP-1 binding of these inhibitors is not yet available.

We therefore carried out the de novo design of cyclic peptides exhibiting AP-1 inhibitory activity using the 3D structure of the bZIP domains from the X-ray crystal structure of the AP-1–DNA complex.[7] Our aim was to construct a hypothetical 3D pharmacophore model for generating new AP-1 inhibitors. A pharmacophore model is defined as the 3D arrangement of the structural and physicochemical features that are relevant to biological activity and is a versatile tool to aid in the discovery and development of new lead compounds.[17]

Cyclization of a flexible linear peptide is known to reduce the conformational freedom of the peptide and restrict its possible conformations, often resulting in

* To whom correspondence should be addressed. Tel: +81-76-431-8218. Fax: +81-76-431-8208. E-mail: KEIICHI_TUCHIDA@toyama-chemical.co.jp.
† Discovery Laboratories, Toyama Chemical Co., Ltd.
‡ Research Laboratories, Toyama Chemical Co., Ltd.
§ Kobe University School of Medicine.
∥ Kobe University Hospital.
⊥ Kitasato University.

10.1021/jm049890+ CCC: $27.50
Published on Web 07/21/2004